Control of Cascaded Multilevel Converters with Unequal Voltage Sources for HEVs

Leon M. Tolbert[1,2], John N. Chiasson[1], Keith J. McKenzie[1] and Zhong Du[1]
[1]ECE Department, The University of Tennessee, Knoxville, TN 37996-2100
tolbert@utk.edu, chiasson@utk.edu, kmc18@utk.edu, zdu1@utk.edu
[2]Power Electronics and Electric Machinery Research Center
Oak Ridge National Laboratory, NTRC, 2360 Cherahala Boulevard, Knoxville, TN 37932

Abstract— **One promising technology to interface battery packs in electric and hybrid electric vehicles is the multilevel converter. In the work presented here, it is shown how the switching times (angles) in a multilevel inverter can be chosen to achieve a required fundamental voltage and not generate specific higher order harmonics. The method gives a complete solution to the problem in that all possible solutions are found.**

Keywords— **Hybrid Electric Vehicles, Multilevel Converters, Harmonic Elimination, Resultants**

I. Introduction

Due to the improved fuel economy offered by hybrid electric vehicles (HEVs), almost all passenger vehicle manufacturers are either producing or plan to produce these models in the near future. With similar fuel economy savings expected in large heavy duty HEVs such as military combat vehicles or large-payload trucks, research has been conducted into different drivetrain configurations that can supply the large power required for these vehicles. One converter topology especially suited to large power ratings and interfacing with multiple dc sources such as the multiple battery modules that may be found on a HEV is the multilevel converter.

Figure 1 is a schematic layout for a cascade multilevel inverter used to interface battery packs to a traction motor in a HEV. Transformerless multilevel inverters are particularly suited for this application because of the high VA ratings possible with these inverters [6]. The multilevel voltage source inverter's unique structure allows it to reach high voltages with low harmonics without the use of transformers or series-connected, synchronized-switching devices. The general function of the multilevel inverter is to synthesize a desired voltage from several levels of DC voltages. For this reason, multilevel inverters can easily provide the high power required of a large electric traction drive.

For parallel-configured HEVs, a cascaded H-bridges inverter can be used to drive the traction motor from a set of batteries, ultracapacitors, or fuel cells. The use of a cascade inverter also allows the HEV drive to continue to operate even with the failure of one level of the inverter structure [10][12][13]. The interest here is a cascade multilevel inverter switching at the fundamental frequency with non equal dc sources. However, many interesting PWM techniques have been proposed for controlling these inverters, for example, [4][7][8][10] where in [4] harmonic elimination was studied by phase shifting the carrier frequency.

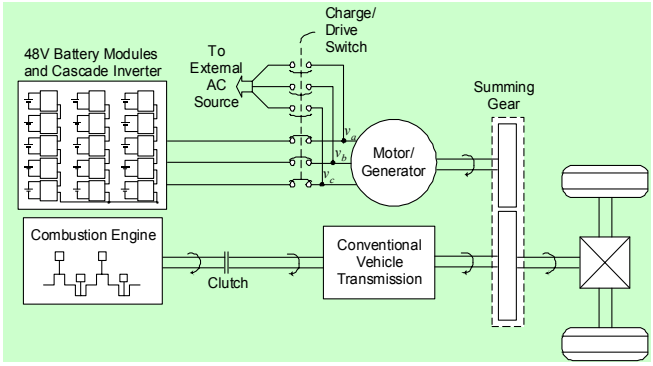

Fig. 1. Schematic layout for a multilevel inverter used in a HEV.

Most previous work with multilevel cascaded inverters assumed all levels had exactly the same voltage or were integer multiples of each other. In this paper, a solution is given where all of the levels are not equal as would likely be the case in an HEV. Specifically, it is shown how the switching times (angles) in a multilevel inverter can be chosen to achieve a required fundamental voltage and not generate specified higher order harmonics. Further, the solution is complete in that *all* possible solutions are found.

II. Cascaded H-bridges

The cascade multilevel inverter consists of a series of H-bridge (single-phase full-bridge) inverter units. The general function of this multilevel inverter is to synthesize a desired voltage from several separate DC sources (SDCSs), which may be obtained from batteries, fuel cells, or ultracapacitors in a HEV. Figure 2 shows a single-phase structure of a cascade inverter with SDCSs [6].

Each SDCS is connected to a single-phase full-bridge inverter. Each inverter level can generate three different voltage outputs, $+V_{dc}, 0$ and $-V_{dc}$ by connecting the DC source to the ac output side by different combinations of the four switches, S_1, S_2, S_3 and S_4. The ac output of each level's full-bridge inverter is connected in series such that the synthesized voltage waveform is the sum of all of the individual inverter outputs.

0-7803-7817-2/03/$17.00 ©2003 IEEE

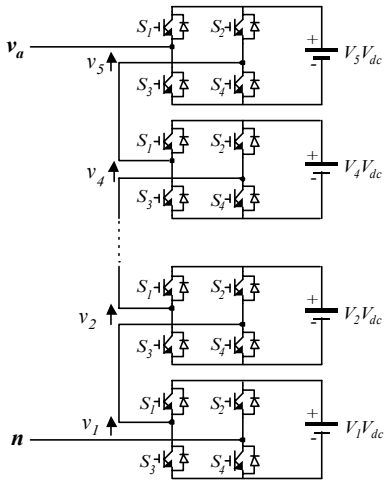

Fig. 2. Single-phase structure of a multilevel cascaded H-bridges inverter.

The number of output phase voltage levels in a cascade multilevel inverter is then $2s+1$, where s is the number of DC sources. An example phase voltage waveform for an 11-level cascaded multilevel inverter with five SDCSs ($s=5$) and five full bridges is shown in Figure 3. The output phase voltage is given by $v_{an} = v_{a1} + v_{a2} + v_{a3} + v_{a4} + v_{a5}$.

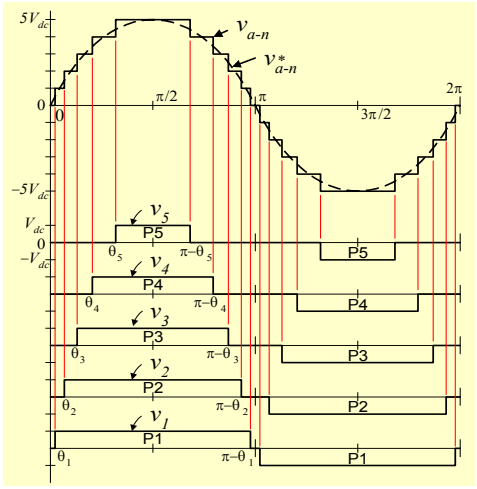

Fig. 3. Output waveform of an 11-level cascade multilevel inverter.

With enough levels and an *appropriate* switching algorithm, the multilevel inverter results in an output voltage that is almost sinusoidal.

III. Mathematical Model of Switching for the Multilevel Converter

The interest here is the case where the separate DC sources do not have equal voltage levels [3]. The Fourier series expansion of the (stepped) output voltage waveform of the multilevel inverter is then given by

$$V(\omega t) = \frac{4V_{dc}}{\pi} \times \sum_{n=1,3,5,\ldots}^{\infty} \frac{1}{n}\Big(V_1\cos(n\theta_1) + \cdots + V_s\cos(n\theta_s)\Big)\sin(n\omega t) \quad (1)$$

where s is the number of DC sources and the *product* V_iV_{dc} is the value of the i^{th} DC source. In particular, if all the DC sources have the same value V_{dc}, then $V_1 = V_2 = \cdots = V_s = 1$. Note also that the number of switching angles was chosen to be the same as the number of levels so that all devices switch at the fundamental frequency. This is not essential to the technique, and one may choose to switch more often to eliminate additional harmonics (e.g., multilevel programmed PWM [1]).

To illustrate the approach, consider a multilevel converter with three DC sources; the switching angles $\theta_1, \theta_2, \theta_3$ are chosen to achieve the desired fundamental voltage while not generating the 5^{th} and 7^{th} order harmonics. The mathematical statement of these conditions is then

$$\begin{aligned} V_1\cos(\theta_1) + V_2\cos(\theta_2) + V_3\cos(\theta_3) &= \frac{\pi V_f}{4V_{dc}} \\ V_1\cos(5\theta_1) + V_2\cos(5\theta_2) + V_3\cos(5\theta_3) &= 0 \\ V_1\cos(7\theta_1) + V_2\cos(7\theta_2) + V_3\cos(7\theta_3) &= 0. \end{aligned} \quad (2)$$

This is a system of 3 transcendental equations in the unknowns $\theta_1, \theta_2, \theta_3$. The first step is to convert the equations (2) to a polynomial system by setting $x_1 = \cos(\theta_1), x_2 = \cos(\theta_2), x_3 = \cos(\theta_3)$ and use the trigonometric identities

$$\begin{aligned} \cos(5\theta) &= 5\cos(\theta) - 20\cos^3(\theta) + 16\cos^5(\theta) \\ \cos(7\theta) &= -7\cos(\theta) + 56\cos^3(\theta) - 112\cos^5(\theta) + 64\cos^7(\theta) \end{aligned}$$

to transform (2) into the equivalent conditions

$$\begin{aligned} p_1(x) &\triangleq V_1x_1 + V_2x_2 + V_3x_3 - m = 0 \\ p_5(x) &\triangleq \sum_{i=1}^{3} V_i\left(5x_i - 20x_i^3 + 16x_i^5\right) = 0 \\ p_7(x) &\triangleq \sum_{i=1}^{3} V_i\left(-7x_i + 56x_i^3 - 112x_i^5 + 64x_i^7\right) = 0 \end{aligned} \quad (3)$$

where $x = (x_1, x_2, x_3)$ and $m \triangleq V_f/\left(4V_{dc}/\pi\right)$.

The system (3) is a set of three *polynomial* equations in the three unknowns x_1, x_2, x_3. Further, the solutions must satisfy $0 \le x_3 \le x_2 \le x_1 \le 1$. As a first step in solving the equations, one substitutes $x_3 = \big(m - (V_1x_1 + V_2x_2)\big)/V_3$ into p_5, p_7 to get

$$\begin{aligned} &p_5(x_1, x_2, V_1, V_2, V_3) = \\ &5x_1 - 20x_1^3 + 16x_1^5 + 5x_2 - 20x_2^2 + 16x_2^5 \\ &+5\left(\frac{m - (V_1x_1 + V_2x_2)}{V_3}\right) - 20\left(\frac{m - (V_1x_1 + V_2x_2)}{V_3}\right)^3 \\ &+16\left(\frac{m - (V_1x_1 + V_2x_2)}{V_3}\right)^5 \end{aligned}$$

and

$$p_7(x_1,x_2,V_1,V_2,V_3) = -7x_1 + 56x_1^3 - 112x_1^5 + 64x_1^7$$
$$-7x_2 + 56x_2^3 - 112x_2^5 + 64x_2^7 - 7\left(\frac{m-(V_1x_1+V_2x_2)}{V_3}\right)$$
$$+56\left(\frac{m-(V_1x_1+V_2x_2)}{V_3}\right)^3 - 112\left(\frac{m-(V_1x_1+V_2x_2)}{V_3}\right)^5$$
$$+64\left(\frac{m-(V_1x_1+V_2x_2)}{V_3}\right)^7.$$

The system of equations $p_5(x_1,x_2,V_1,V_2,V_3) = 0$, $p_7(x_1,x_2,V_1,V_2,V_3) = 0$ are now two polynomials in the two unknowns x_1, x_2 that must be solved.

A. Solving Polynomial Equations

In order to explain how one computes the zero sets of polynomial systems, a brief discussion of the procedure of solving such systems is now given. A systematic procedure to do this is known as *elimination theory* and uses the notion of *resultants* [2][5]. Briefly, one considers $a(x_1,x_2)$ and $b(x_1,x_2)$ as polynomials in x_2 whose coefficients are polynomials in x_1. Then, for example, letting $a(x_1,x_2)$ and $b(x_1,x_2)$ have degrees 3 and 2, respectively in x_2, they may be written in the form

$$\begin{aligned} a(x_1,x_2) &= a_3(x_1)x_2^3 + a_2(x_1)x_2^2 + a_1(x_1)x_2 + a_0(x_1) \\ b(x_1,x_2) &= b_2(x_1)x_2^2 + b_1(x_1)x_2 + b_0(x_1). \end{aligned}$$

The $n \times n$ *Sylvester* matrix, where $n = \deg_{x_2}\{a(x_1,x_2)\} + \deg_{x_2}\{b(x_1,x_2)\} = 3+2 = 5$, is defined by

$$S_{a,b}(x_1) = \begin{bmatrix} a_0(x_1) & 0 & b_0(x_1) & 0 & 0 \\ a_1(x_1) & a_0(x_1) & b_1(x_1) & b_0(x_1) & 0 \\ a_2(x_1) & a_1(x_1) & b_2(x_1) & b_1(x_1) & b_0(x_1) \\ a_3(x_1) & a_2(x_1) & 0 & b_2(x_1) & b_1(x_1) \\ 0 & a_3(x_1) & 0 & 0 & b_2(x_1) \end{bmatrix}.$$

The *resultant* polynomial is then defined by

$$r(x_1) = \mathrm{Res}\left(a(x_1,x_2), b(x_1,x_2), x_2\right) \triangleq \det S_{a,b}(x_1) \quad (4)$$

and is the result of solving $a(x_1,x_2) = 0$ and $b(x_1,x_2) = 0$ simultaneously for x_1, i.e., eliminating x_2. See the Appendix for a detailed discussion on resultants.

IV. Solution of the Harmonic Elimination Equations

As briefly explained, the theory of resultants provides a systematic method to find the polynomial $r(x_1,V_1,V_2,V_3) \triangleq \mathrm{Res}(p_5,p_7,x_2)$ that results when x_2 is eliminated by simultaneously solving $p_5(x_1,x_2,V_1,V_2,V_3) = 0$, $p_7(x_1,x_2,V_1,V_2,V_3) = 0$. One then numerically computes the roots of $r(x_1,V_1,V_2,V_3) = 0$ for the roots $\{x_{1i}, i = 1,...,n_1 = \deg_{x_1}\{r(x_1,V_1,V_2,V_3)\}\}$. Each of the roots x_{1i} are substituted back into $p_5(x_1,x_2), p_7(x_1,x_2)$ and then the polynomials $p_5(x_{1i},x_2,V_1,V_2,V_3) = 0$, $p_7(x_{1i},x_2,V_1,V_2,V_3) = 0$ are each solved (numerically) for x_2. Their common roots $\{x_{2ij}, j = 1,...,n_2\}$ are used to get the pairs (x_{1i},x_{2ij}) that satisfy the original system.

This algorithm was used to find the switching angles for each phase in a multilevel inverter with non equal DC sources. The results for phase a are plotted in Figure 4 where DC source voltages for this phase were measured to be $V_1V_{dc} = 60.0$ V, $V_2V_{dc} = 47.0$ V and $V_3V_{dc} = 43.1$ V.

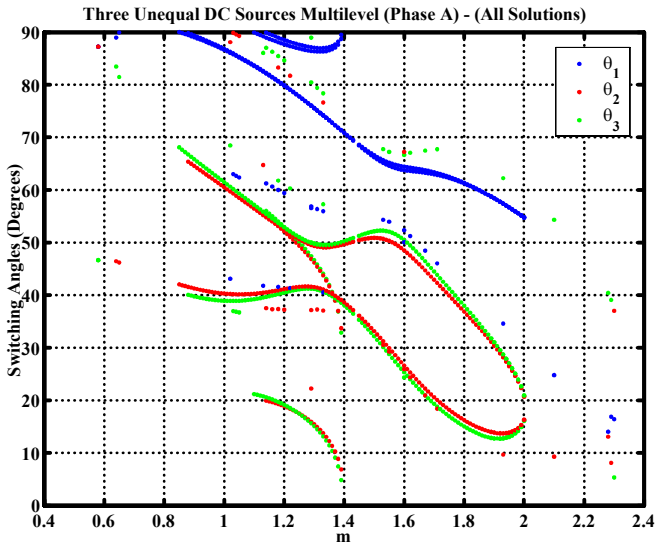

Fig. 4. All solution sets $\{\theta_1,\theta_2,\theta_3\}$ vs. m

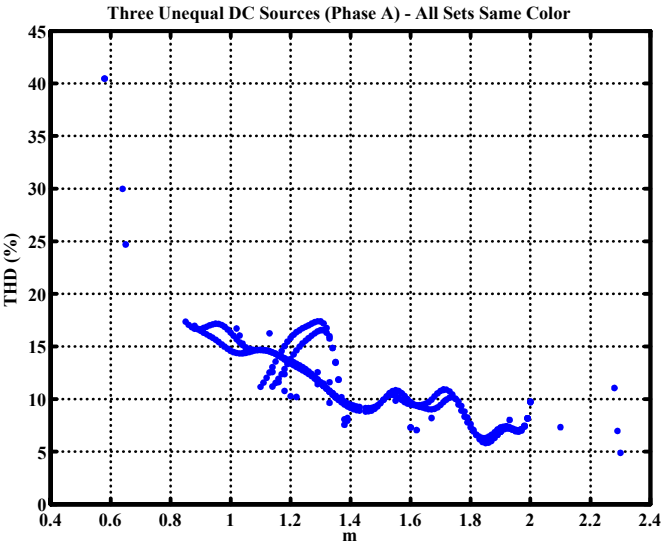

Fig. 5. Total harmonic distortion vs. m for all possible switching angles solutions.

It is important to note that the interest here is in a *symbolic* expression for the final resultant polynomial. That is, the final resultant polynomial is more precisely written as $r(x_1,m,V_{dc1},V_{dc2},V_{dc3})$ showing that not only is it a function of the indeterminate x_1, but also of the parameters $m, V_{dc1}, V_{dc2}, V_{dc3}$. This is the desired form because, for example, in a hybrid electric vehicle the batteries powering the vehicle will not usually be at the same voltage level and will vary with use. Consequently, the DC source

voltages could be measured and the switching angles (such as those shown in Figure 4) could be recomputed *online* to account for changes in the source voltages. Figure 4 shows the switching angles $\theta_1, \theta_2, \theta_3$ vs. m for those values of m in which the system (2), or equivalently (3), has at least one solution set. The parameter m was incremented in steps of 0.01. Note that for m in the range from approximately 1.1 to 2.4, there are at least two different sets of solutions and sometimes three sets. One clear way to choose a particular solution is simply to pick the one that results in the smallest total harmonic distortion (THD) given by

$$THD = \sqrt{\left(V_5^2 + V_7^2 + V_{11}^2 + V_{13}^2 + V_{17}^2 + \cdots + V_{31}^2\right)/V_1^2}.$$

This is shown in Figure 5 corresponding to the solutions given in Figure 4.

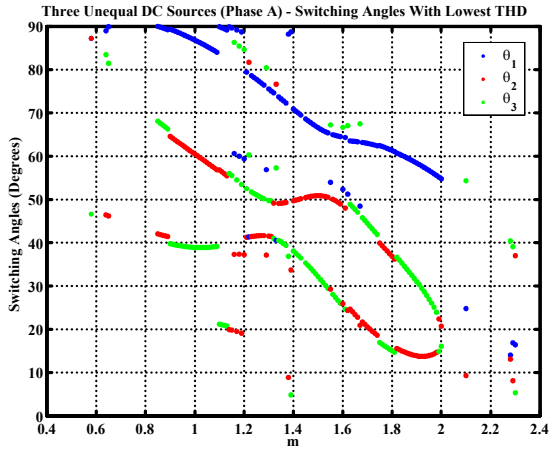

Fig. 6. Solution set $\{\theta_1, \theta_2, \theta_3\}$ vs. m that gives the smallest possible THD

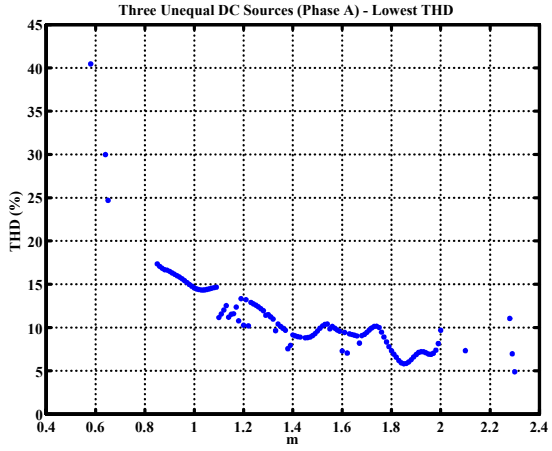

Fig. 7. Total harmonic distortion vs. m for the switching angles that result in the smallest THD.

Choosing the switching angles based on this criteria, the multiple switching angle solutions given in Figure 4 reduce to the single set of solutions given in Figure 6, and the corresponding THD is shown in Figure 7. If V_1, V_2, V_3 are given (measured), the computation of the complete set switching angles vs m as in Figure 6 takes less than minute in MATLAB. Consequently, by monitoring the voltages of the separate DC sources, the switching angles can be updated online as the source voltages vary.

V. Experimental Work

A prototype three-phase 11-level wye-connected cascaded inverter has been built using 100 V, 70 A MOSFETs as the switching devices. The gate driver boards and MOSFETs are shown in Figure 8. A battery bank of 15 SDCSs of 60 Volts DC (nominally) each feed the inverter configured with 5 SDCSs per phase [11]. In the experimental study here, this prototype system was configured to be 7-levels (3 SDCSs per phase).

Fig. 8. Gate Driver Boards and MOSFETs for the Mulitlevel Inverter

The ribbon cable shown in the figure provides the communication link between the gate driver board and the real-time processor. In this work, a real-time computing platform [9] was used to interface the computer (which generates the logic signals) to this cable. This system allows one to implement the switching algorithm as a lookup table in SIMULINK which is then converted to C code using RTW (real-time workshop) from *Mathworks*. The software provides icons to interface the SIMULINK model to the digital I/O board and converts the C code into executables.

The time resolution (the precision for the time at which a switch is turned on or off) was chosen to be 1/1000 of an electrical cycle. For a 60 Hz frequency requirement, this comes to $(1/60)/1000 = 16.7$ microseconds. The real-time implementation is accomplished by putting the data (i.e., Figure 6) in a lookup table and therefore does not require high computational power for implementation. As the voltage levels change, the stored resultant polynomial $r(x_1, m, V_{dc1}, V_{dc2}, V_{dc3})$ can be updated and the table of switching angles recomputed online in the order of a few seconds. In contrast, if iterative numerical techniques are used, one is not guaranteed that the solution will converge (the initial guess has to be "close" to the solution or there may be no solution), nor that the particular solution obtained is the only solution and, therefore, the best in any

sense. The multilevel converter was attached to a three phase induction motor with the following nameplate data:

Rated hp	=	1/3 hp
Rated Current	=	1.5 A
Rated Speed	=	1725 rpm
Rated Voltage	=	208 V (RMS line-to-line @ 60 Hz)

The voltage for each separate DC source of each phase was measured and is given in the table below.

Phase	V_1V_{dc}	V_2V_{dc}	V_3V_{dc}
a	60.0 V	47.0 V	43.1 V
b	59.9 V	48.4 V	43.1 V
c	60.1 V	47.3 V	41.4 V

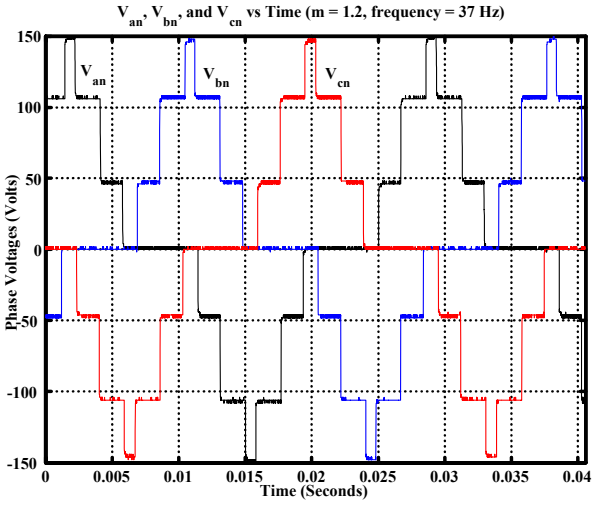

Fig. 9. Three phase voltage waveforms for m $m_a = 0.4$ ($m = 1.2$).

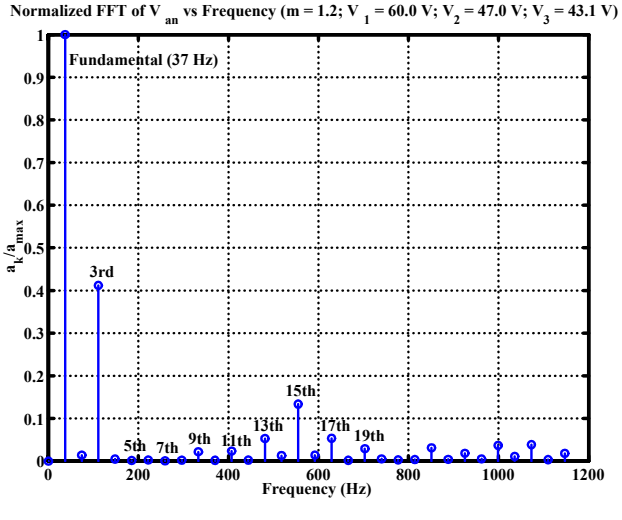

Fig. 10. Fast Fourier transform of the phase a voltage shown in Figure 9.

In the first set of experiments, the parameter m was set equal to 1.2 (for a modulation index $m_a = 1.2/3 = 0.4$) and the frequency set to 37 Hz. The switching angles for phase a were taken from Figure 6 with $m = 1.2$ while a similar computation was done to obtain the switching angles for phases b and c. The resulting three phase voltages were measured and are shown in Figure 9 (The spikes on the plot are due to the low bit resolution of the sampling scope and are not present on the actual scope display). The FFT of the voltage waveform of phase a is shown in Figure 10. Note that the 5^{th} and 7^{th} harmonics are zero as predicted. The phase currents in the motor produced by the voltages of Figure 9 are shown in Figure 11. The FFT of the current waveform of phase a is shown in Figure 12. Note that the harmonic content of the current is significantly reduced compared to harmonic content of the voltage due to filtering by the motor's inductance. The THD for the current waveform of phase a was found to be 4.8%.

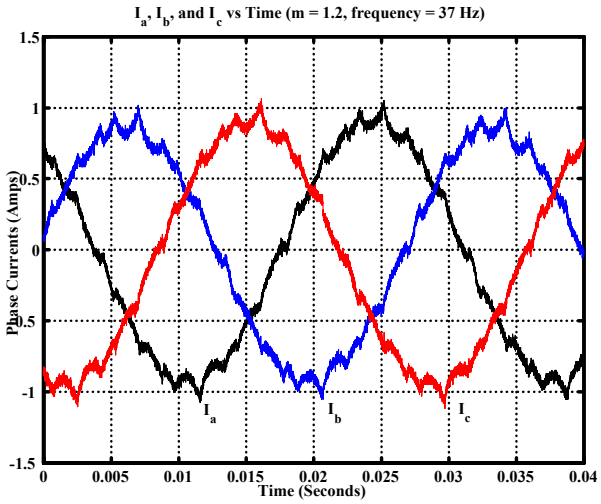

Fig. 11. Phase currents vs. time in seconds for $m_a = 0.4$ ($m = 1.2$).

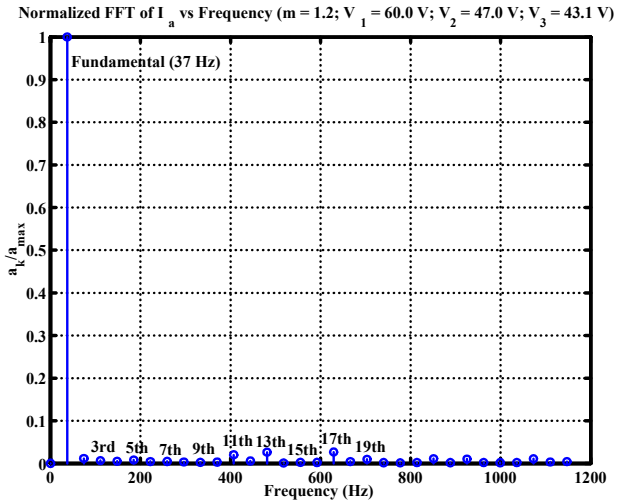

Fig. 12. Normalized FFT of the phase a current shown in Figure 11.

In the second set of experiments, the parameter m was set equal to 1.95 (for a modulation index $m_a = 1.95/3 =$

0.65) and the frequency set to 60 Hz. The switching angles for phase a were again taken from Figure 6 with $m = 1.95$ while a similar computation was done to obtain the switching angles for phases b and c. The three phase voltages applied to the motor are shown in Figure 13, and the FFT of the voltage waveform of phase a is given in Figure 14. Note that the 5^{th} and 7^{th} harmonics are zero as predicted.

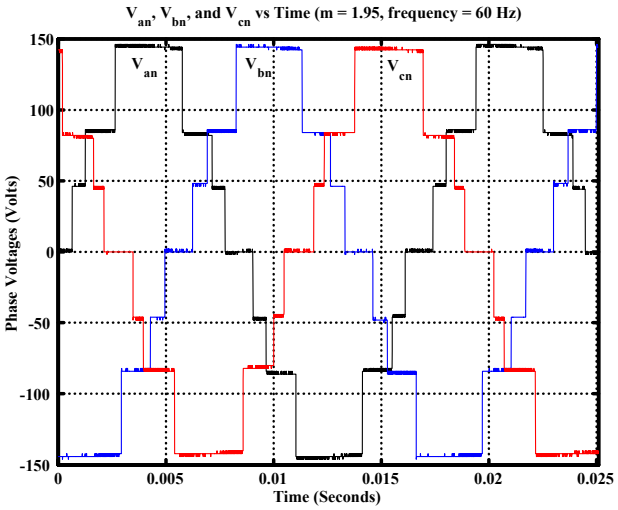

Fig. 13. Three phase voltage waveforms for $m_a = 0.65$ ($m = 1.95$).

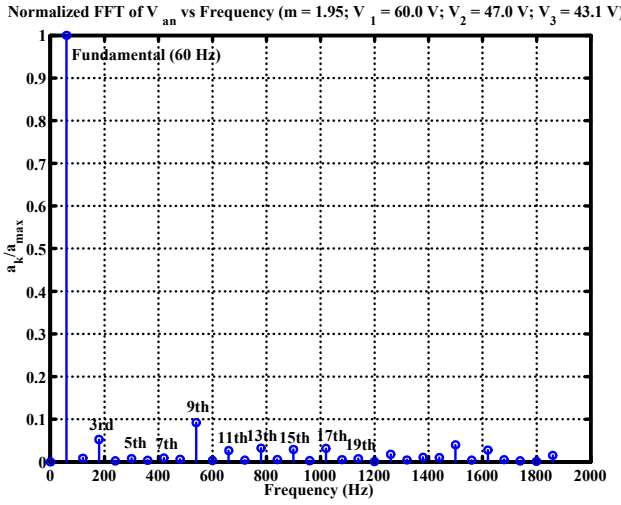

Fig. 14. Normalized FFT of the phase a voltage waveform of Figure 13.

Figure 15 shows the three phase motor currents resulting from applying the voltages of Figure 13 to the motor. The FFT of the current waveform of phase a is shown in Figure 16. Again, the harmonic content of the current is significantly reduced compared to harmonic content of the voltage due to filtering by the motor's inductance.

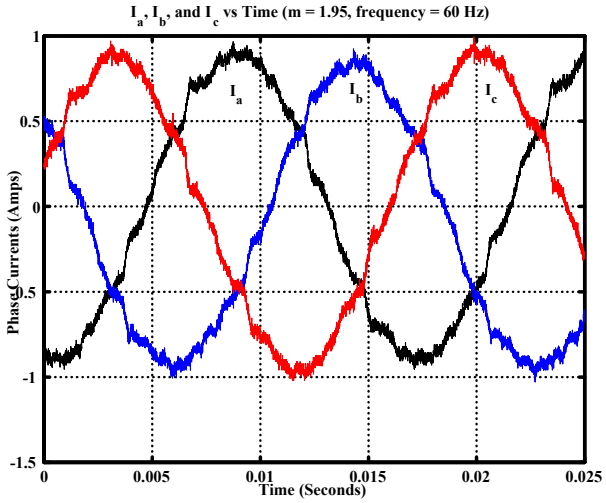

Fig. 15. Current waveforms for $m_a = 0.65$ ($m = 1.95$).

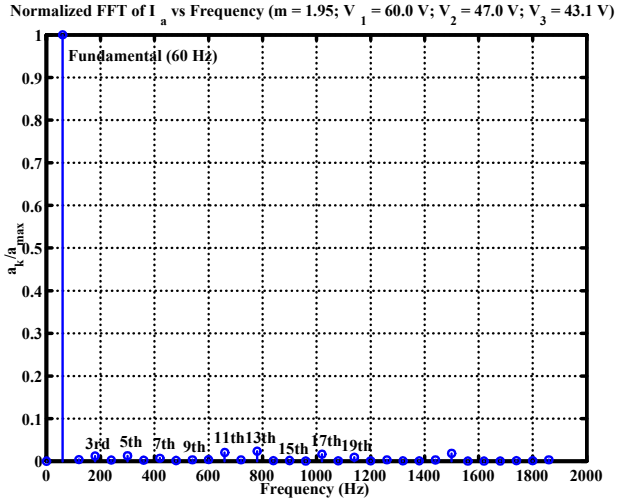

Fig. 16. Fast Fourier transform of the phase a current waveform shown in Figure 15.

The THD for the current waveform of phase a was computed using the FFT data of Figure 16 and was found to be 4.15%.

VI. Conclusions

Elimination theory and the notion of resultants can be used to eliminate the lower order harmonics in a multilevel converter that has non equal DC sources. This method is expected to be particularly useful for HEV applications as one would not expect the battery packs to be able to maintain equal DC voltages. Future research includes extending this to the case when there are more than three DC sources and methods to balance the DC sources against unequal discharge rates.

VII. Acknowledgements

Dr. Tolbert would like to thank the National Science Foundation for partially supporting this work through con-

tract NSF ECS-0093884. Drs. Chiasson and Tolbert would like to thank Oak Ridge National Laboratory (especially Don Adams) for partially supporting this work through the UT-Battelle contract number 4000007596. The University of Tennessee is gratefully acknowledged for providing funding for the equipment in this project through its SARIF program. Finally, the authors would like to also thank Opal-RT Technologies for their courteous and professional help in support of this project.

References

[1] J. Chiasson, L. M. Tolbert, K. McKenzie, and Z. Du. A complete solution to the harmonic elimination problem. In *Proceedings of Applied Power Electronics Conference APEC 2003*, pages 596–602, February 2003. Miami FL.

[2] D. Cox, J. Little, and D. O'Shea. *IDEALS, VARIETIES, AND ALGORITHMS An Introduction to Computational Algebraic Geometry and Commutative Algebra, Second Edition*. Springer-Verlag, 1996.

[3] T. Cunnyngham. Cascade multilevel inverters for large hybrid-electric vehicle applications with variant DC sources. Master's thesis, The University of Tennessee, 2001.

[4] D. G. Holmes and B. P. McGrath. Opportunities for harmonic cancellation with carrier-based pwm for two-level and multilevel cascaded inverters. *IEEE Transactions on Industry Applications*, 37(2):574–582, March/April 2001.

[5] Joachim von zur Gathen and Jürgen Gerhard. *Modern Computer Algebra*. Cambridge University Press, 1999.

[6] J. S. Lai and F. Z. Peng. Multilevel converters - A new breed of power converters. *IEEE Transactions on Industry Applications*, 32(3):509–517, May/June 1996.

[7] R. Lund, M. D. Manjrekar, P. Steimer, and T. A. Lipo. Control strategies for a hybrid seven inverter. In *Proceedings of the European Power Electronic Conference*, September 1999. Lausanne Switzerland.

[8] M. Manjrekar and T. Lipo. A hybrid multilevel inverter topology for drive applications. In *Proceedings of the Applied Power Electronic Conference*, pages 523–529, February 1998. Anaheim CA.

[9] Opal-RT Technologies. RTLab. 2001. See http://www.opal-rt.com/.

[10] L. M. Tolbert and T. G. Habetler. Novel multilevel inverter carrier-based PWM methods. *IEEE Transactions on Industry Applications*, 35(5):1098–1107, Sept./Oct. 1999.

[11] L. M. Tolbert, F. Z. Peng, T. Cunnyngham, and J. Chiasson. Charge balance control schemes for cascade multilevel converter in hybrid electric vehicles. *IEEE Transactions on Industrial Electronics*, 49(5):1058–1064, October 2002.

[12] L. M. Tolbert, F. Z. Peng, and T. G. Habetler. Multilevel converters for large electric drives. *IEEE Transactions on Industry Applications*, 35(1):36–44, Jan./Feb. 1999.

[13] L. M. Tolbert, F. Z. Peng, and T. G. Habetler. Multilevel PWM methods at low modulation indexes. *IEEE Transactions on Power Electronics*, 15(4):719–725, July 2000.

Appendix

A. Resultants

Given two polynomials $a(x_1, x_2)$ and $b(x_1, x_2)$ how does one find their common zeros? That is, the values (x_{10}, x_{20}) such that

$$a(x_{10}, x_{20}) = b(x_{10}, x_{20}) = 0.$$

Consider $a(x_1, x_2)$ and $b(x_1, x_2)$ as polynomials in x_2 whose coefficients are polynomials in x_1. For example, let $a(x_1, x_2)$ and $b(x_1, x_2)$ have degrees 3 and 2, respectively in x_2 so that they may be written in the form

$$\begin{aligned} a(x_1, x_2) &= a_3(x_1)x_2^3 + a_2(x_1)x_2^2 + a_1(x_1)x_2 + a_0(x_1) \\ b(x_1, x_2) &= b_2(x_1)x_2^2 + b_1(x_1)x_2 + b_0(x_1). \end{aligned}$$

In general, there is always a polynomial $r(x_1)$ (called the *resultant polynomial*) such that

$$\alpha(x_1, x_2)a(x_1, x_2) + \beta(x_1, x_2)b(x_1, x_2) = r(x_1).$$

So if $a(x_{10}, x_{20}) = b(x_{10}, x_{20}) = 0$ then $r(x_{10}) = 0$, that is, if (x_{10}, x_{20}) is a common zero of the pair $\{a(x_1, x_2), b(x_1, x_2)\}$, then the first coordinate x_{10} is a zero of $r(x_1) = 0$. The roots of $r(x_1)$ are easy to find (numerically) as it is a polynomial in one variable. To find the common zeros of $\{a(x_1, x_2), b(x_1, x_2)\}$, one computes all roots x_{1i} $i = 1, ..., n_1$ of $r(x_1)$. Next, for each such x_{1i}, one (numerically) computes the roots of

$$a(x_{1i}, x_2) = 0 \tag{5}$$

and the roots of

$$b(x_{1i}, x_2) = 0. \tag{6}$$

Any root x_{2j} that is in the solution set of both (5) and (6) for a given x_{1i} results in the pair (x_{1i}, x_{2j}) being a common zero of $a(x_1, x_2)$ and $b(x_1, x_2)$. Thus, this gives a method of solving polynomials in one variable to compute the common zeros of $\{a(x_1, x_2), b(x_1, x_2)\}$.

To see how one obtains $r(x_1)$, let

$$\begin{aligned} a(x_1, x_2) &= a_3(x_1)x_2^3 + a_2(x_1)x_2^2 + a_1(x_1)x_2 + a_0(x_1) \\ b(x_1, x_2) &= b_2(x_1)x_2^2 + b_1(x_1)x_2 + b_0(x_1) \end{aligned}$$

Next, see if polynomials of the form

$$\begin{aligned} \alpha(x_1, x_2) &= \alpha_1(x_1)x_2 + \alpha_0(x_1) \\ \beta(x_1, x_2) &= \beta_2(x_1)x_2^2 + \beta_1(x_1)x_2 + \beta_0(x_1). \end{aligned}$$

can be found such that

$$\alpha(x_1, x_2)a(x_1, x_2) + \beta(x_1, x_2)b(x_1, x_2) = r(x_1). \tag{7}$$

Equating powers of x_2, this equation may be rewritten in matrix form as

$$\begin{bmatrix} a_0 & 0 & b_0 & 0 & 0 \\ a_1 & a_0 & b_1 & b_0 & 0 \\ a_2 & a_1 & b_2 & b_1 & b_0 \\ a_3 & a_2 & 0 & b_2 & b_1 \\ 0 & a_3 & 0 & 0 & b_2 \end{bmatrix} \begin{bmatrix} \alpha_0(x_1) \\ \alpha_1(x_1) \\ \beta_0(x_1) \\ \beta_1(x_1) \\ \beta_2(x_1) \end{bmatrix} = \begin{bmatrix} r(x_1) \\ 0 \\ 0 \\ 0 \\ 0 \end{bmatrix}$$

The matrix on the left-hand side is called the *Sylvester* matrix and is denoted here by $S_{a,b}(x_1)$. The inverse of $S_{a,b}(x_1)$ has the form

$$S_{a,b}^{-1}(x_1) = \frac{1}{\det S_{a,b}(x_1)} \text{adj}\left(S_{a,b}(x_1)\right)$$

where $\text{adj}(S_{a,b}(x_1))$ is the adjoint matrix and is a 5×5 *polynomial* matrix in x_1. Solving for $\alpha_i(x_1), \beta_i(x_1)$ gives

$$\begin{bmatrix} \alpha_0(x_1) \\ \alpha_1(x_1) \\ \beta_0(x_1) \\ \beta_1(x_1) \\ \beta_2(x_1) \end{bmatrix} = \frac{\text{adj}S_{a,b}(x_1)}{\det S_{a,b}(x_1)} \begin{bmatrix} r(x_1) \\ 0 \\ 0 \\ 0 \\ 0 \end{bmatrix}.$$

Choosing $r(x_1) = \det S_{a,b}(x_1)$ this becomes

$$\begin{bmatrix} \alpha_0(x_1) \\ \alpha_1(x_1) \\ \beta_0(x_1) \\ \beta_1(x_1) \\ \beta_2(x_1) \end{bmatrix} = \text{adj}S_{a,b}(x_1) \begin{bmatrix} 1 \\ 0 \\ 0 \\ 0 \\ 0 \end{bmatrix}$$

and guarantees that $\alpha_0(x_1), \alpha_1(x_1), \beta_0(x_1), \beta_1(x_1), \beta_2(x_1)$ are polynomials in x_1. That is, the *resultant polynomial* defined by $r(x_1) = \det S_{a,b}(x_1)$ is the polynomial required for (7).